JOURNAL OF SOLID STATE CHEMISTRY 62, 371–376 (1986)

Structure of Dichromate-Type Lead Pyrophosphate, $Pb_2P_2O_7$

D. F. MULLICA, HERBERT O. PERKINS, AND DAVID A. GROSSIE

Departments of Chemistry and Physics, Baylor University, Waco, Texas 76798

AND L. A. BOATNER AND B. C. SALES

Solid State Division, Oak Ridge National Laboratory, Oak Ridge, Tennessee 38731*

Received June 11, 1985; in revised form September 23, 1985

Lead pyrophosphate, $Pb_2P_2O_7$, crystallizes in the triclinic space group $P\bar{1}$ ($Z = 4$) with $a = 6.914(2)$, $b = 6.966(2)$, $c = 12.751(4)$ Å; $\alpha = 96.82(3)$, $\beta = 91.14(3)$, $\gamma = 89.64(3)°$; and $V = 612.0(6)$ Å^3. Structural refinement data were collected using an automated diffractometer with Mo$K\alpha$ radiation. The lead pyrophosphate structure was refined by a full matrix to an R of 0.069 ($R_w = 0.067$) using 2637 unique reflections. The structure has two unique diphosphate groups that are repeated by lattice translations to form sheets of diphosphate groups. The P_2O_7 groups, dichromate type, are eclipsed to within 9.4 and 13.5°. The Pb^{2+} ions are eight- and nine-coordinated to oxygen atoms with average experimental interatomic distances of 2.695 and 2.767 Å, respectively.

Introduction

Compounds with compositions of the type $X_2Y_2O_7$ provide an illustration of the important role that cation size plays in determining the structural properties of crystals (*1*). Three structural classes, determined by the ionic radii of both the X and Y atoms, have been described for these materials (*2*). Crystals in which the ionic radius of the Y atom is greater than 0.6 Å crystallize in the atopite-type structure where the Y atoms are octahedrally coordinated. When the ionic radius of the Y atom is less than 0.6 Å and the ionic radius of the X atom is less than 0.97 Å, the thortveitite-type structure is realized. If the X atom has a radius greater than 0.97 Å, crystallization with the dichromate-type structure occurs. The coordination number of the Y atom is 4 in both the dichromate- and thortveitite-type structures. The Y_2O_7 anion consists of two tetrahedral YO_4 groups sharing an oxygen atom with a Y–O–Y angle of approximately 130° in the dichromate-type structure and between 139 and 156° in the thortveitite-type structure. The oxygen atoms of the Y_2O_7 group lie in a staggered conformation about the Y–Y axis in the thortvetite structure. The X atom in dichromate-type compounds is usually a large metal atom found in groups I and II (e.g., rubidium, potassium, strontium, calcium, and cadmium) and the Y atom is generally from group V or VI (e.g., phosphorus, vanadium, or sulfur).

* Research sponsored by the Division of Materials Sciences, U.S. Department of Energy, under Contract DE-AC05-840R21400 with Martin Marietta Energy Systems, Inc.

0022-4596/86 $3.00

Representative members of the thortveitite group are zinc and magnesium pyroarsenate (*2*), cadmium pyrovanadate (*3*), and the lanthanide pyrosilicates (*4*). The dichromate-type structure, which has been well described by Brown and Calvo (*1*), includes alkali dichromates (*5*), β-strontium and lead pyrovanadate (*6, 7*), and many pyrophosphates (*8–10*).

Brixner *et al.* (*11*) have previously reported the crystal growth, properties, and X-ray powder diffraction data of lead pyrophosphate. The detailed single-crystal structural analysis of lead pyrophosphate presented in the current work is of interest because this compound is perhaps the closest crystalline analog of an unusual family of amorphous materials (i.e., lead–iron phosphate glasses). The local structural properties of crystalline lead pyrophosphate should bear some relationship to those of the disordered lead–iron phosphate (and lead phosphate) glasses. Accordingly, it is hoped that a complete understanding of the atomic structure of crystalline lead pyrophosphate will provide some insight into the microscopic origin of the unusual physical and chemical characteristics exhibited by lead–iron phosphate glasses (*12*). These glasses have considerable potential technological importance in the area of nuclear waste disposal (*13–15*) as well as in other promising areas of application.

Experimental

Single crystals of lead pyrophosphate were prepared by slowly cooling a molten mixture of high-purity PbO (99.999% from Johnson–Matthey, Inc.) and P_2O_5 (added as $NH_4H_2PO_4$, 99.999%, from Johnson–Matthey, Inc.). A stoichiometric (1 : 1) combination of PbO and $NH_4H_2PO_4$ powders was thoroughly mixed together and placed in a 50-cc Pt crucible. The powder was slowly heated to 500°C and held at this temperature for 1 hr to ensure the complete decomposition of $NH_4H_2PO_4$ to P_2O_5 (with the evolution of water vapor and ammonia gas). After the mixture was heated to 1000°C in air [i.e., about 170°C above the melting point of lead pyrophosphate (*11*)], the molten liquid was repeatedly stirred to ensure compositional homogeneity throughout the melt. The melt temperature was then reduced to 900°C, followed by a slow cooling of the melt (about 2°C/min) to 750°C. At 750°C, the oven power was turned off and the solidified melt was allowed to cool to room temperature at the natural cooling rate of the oven (about 1–2°C/min). Optically clear lead pyrophosphate single-crystal plates measuring about $5 \times 5 \times 1$ mm^3 could be easily removed from the solidified melt. Energy-dispersive X-ray analysis and powder X-ray diffraction analysis indicated that the crystals had the proper lead-to-phosphorus ratio and a powder pattern which was very similar to that previously reported by Brixner *et al.* (*11*).

Diffraction data were collected using an Enraf–Nonius CAD-4F diffractometer and a clear colorless $Pb_2P_2O_7$ crystal measuring $0.168 \times 0.336 \times 0.360$ mm. Graphite monochromized Mo$K\alpha$ ($\bar{\lambda} = 0.71073$ Å) radiation was used. Lattice constants and the orientation matrix were obtained through a least-squares refinement of 25 accurately centered reflections. The lattice parameters are $a = 6.941(2)$, $b = 6.966(2)$, $c = 12.751(4)$ Å; $\alpha = 96.82(3)$, $\beta = 91.14(3)$, and $\gamma = 89.64(3)°$. Intensity data were collected using the ω-2θ technique with a variable scan rate (0.38–3.35° min^{-1}) determined by a fast prescan of 3.35° min^{-1}. Data were collected in the range $3 < 2\theta < 60°$. Two standard reflections ($4\bar{1}5$ and $1\bar{4}\bar{2}$) were monitored every 2 hr of collection time and revealed only random intensity variations (<1.1%). Lorentz, polarization, and absorption corrections ($\mu = 588.8$ cm^{-1}) were applied to the data. Equivalent reflections were aver-

TABLE I

EXPERIMENTAL AND STATISTICAL SUMMARY

a = 6.941(2) Å	Triclinic
b = 6.966(2)	Space group: $P\bar{1}$
c = 12.751(4)	Crystal size: 0.168 × 0.336 × 0.360 mm
α = 96.82(3)°	μ(Mo$K\alpha$) = 558.8 cm^{-1}
β = 91.14(3)	Transition range = 0.0016–0.0446
γ = 89.64(3)	R_{int} = 0.038
V = 612.0(6) Å^3	Δr = 1.5–30°
M_r = 588.32	Unique reflections [$I > 3\sigma(I)$]: 2637
dc = 6.384 Mg m^{-3}	R = 0.069, R_w = 0.067
Z = 4	Max shift/error = 0.0015
$F(000)$ = 1000 e	g = 4.15(11) × 10^{-7} e^{-2}

aged (R_{int} = 0.038), yielding 3332 unique reflections, of which 2637 had intensities greater than 3σ.

Normalized structure factors $|E_{hkl}|$ were obtained by direct methods (MULTAN 11/82) (*16*). Phases of 273 strong reflections with $|E| > 1.2$ were determined. The best solution determined by the summary of figures of merit was expanded to yield the four Pb atoms in the asymmetric unit, space group $P\bar{1}$. Phosphorous and oxygen atoms were located by difference Fourier techniques, using the Pb atoms to phase the electron density map. A full matrix least-

TABLE II

ATOMIC POSITIONAL PARAMETERS (Pb, P × 10^4, AND O × 10^3) AND ISOTROPIC THERMAL PARAMETERS (×10^3) FOR LEAD PYROPHOSPHATE

Atom	x	y	z	U^a
Pb(1)	2460(2)	2046(2)	6498(1)	82(2)
Pb(2)	6729(2)	2105(2)	8600(1)	92(2)
Pb(3)	10910(2)	8111(2)	8528(1)	93(2)
Pb(4)	6524(2)	6240(2)	6334(1)	81(2)
P(1)	2333(11)	8969(10)	4000(7)	55(14)
P(2)	1850(11)	6976(11)	5898(7)	65(14)
P(3)	8346(11)	6988(10)	10859(7)	54(14)
P(4)	5793(11)	7070(11)	8987(7)	57(14)
O(1)	87(3)	920(3)	313(2)	131(47)
O(2)	391(3)	763(3)	361(2)	81(42)
O(3)	305(3)	1089(3)	464(2)	122(46)
O(4)	112(3)	787(3)	485(2)	103(44)
O(5)	17(4)	636(3)	641(2)	166(51)
O(6)	300(3)	855(3)	657(2)	97(44)
O(7)	313(3)	525(3)	548(2)	110(45)
O(8)	992(3)	819(3)	1043(2)	112(45)
O(9)	919(3)	535(3)	1138(2)	103(44)
O(10)	700(3)	830(3)	1155(2)	82(42)
O(11)	706(3)	608(3)	987(2)	79(41)
O(12)	704(4)	854(4)	855(2)	175(52)
O(13)	402(3)	797(3)	955(2)	109(44)
O(14)	525(3)	539(3)	818(2)	120(46)

[a] Pb atoms were refined anisotropically and are given in the form of the isotropic equivalent thermal parameter: $U_{eq} = (U_{11} + U_{22} + U_{33} + U_{12} \cos\gamma + U_{13} \cos\beta + U_{23} \cos\alpha)/3$.

TABLE III

BOND DISTANCES (Å) AND ANGLES (°) FOR LEAD PYROPHOSPHATE

i $-x, 1-y, 1-z$
ii $1-x, 1-y, 1-z$
iii $x, y-1, z$
iv $1-x, 1-y, 2-z$
v $2-x, 1-y, 2-z$
vi $x+1, y, z$
vii $2-x, 2-y, 2-z$
viii $1-x, 2-y, 1-z$

Pb(1)–O(1)^{i}	2.548(13)	Pb(3)–O(1)^{vii}	3.213(13)
Pb(1)–O(2)^{ii}	2.537(13)	Pb(3)–O(5)^{vi}	2.864(15)
Pb(1)–O(3)^{iii}	2.454(14)	Pb(3)–O(6)^{vi}	2.962(13)
Pb(1)–O(4)^{i}	2.994(13)	Pb(3)–O(8)	2.523(14)
Pb(1)–O(6)^{iii}	2.475(12)	Pb(3)–O(8)^{vii}	2.821(13)
Pb(1)–O(7)	2.756(13)	Pb(3)–O(9)^{v}	2.434(12)
Pb(1)–O(9)^{iv}	3.299(14)	Pb(3)–O(10)^{vii}	2.912(12)
Pb(1)–O(10)^{iv}	2.552(13)	Pb(3)–O(12)	2.698(15)
		Pb(3)–O(13)^{vi}	2.505(13)
Pb(2)–O(1)^{ii}	2.850(14)		
Pb(2)–O(2)^{ii}	2.868(13)	Pb(4)–O(2)^{ii}	2.728(12)
Pb(2)–O(8)^{v}	2.631(13)	Pb(4)–O(3)^{viii}	2.495(13)
Pb(2)–O(9)^{v}	3.345(13)	Pb(4)–O(5)^{vi}	2.530(14)
Pb(2)–O(10)^{iv}	2.603(12)	Pb(4)–O(6)	2.922(13)
Pb(2)–O(11)	3.044(13)	Pb(4)–O(7)	2.633(13)
Pb(2)–O(12)^{iii}	2.484(14)	Pb(4)–O(7)^{ii}	2.435(14)
Pb(2)–O(13)^{iv}	2.432(14)	Pb(4)–O(12)	3.096(15)
Pb(2)–O(14)	2.614(13)	Pb(4)–O(14)	2.669(14)
P(1)–O(1)	1.509(14)	O(1)–P(1)–O(2)	110.8(8)
P(1)–O(2)	1.488(13)	O(1)–P(1)–O(3)	115.4(8)
P(1)–O(3)	1.562(14)	O(1)–P(1)–O(4)	103.5(7)
P(1)–O(4)	1.647(14)	O(2)–P(1)–O(3)	113.9(7)
		O(2)–P(1)–O(4)	107.0(7)
P(2)–O(4)	1.613(14)	O(3)–P(1)–O(4)	105.1(7)
P(2)–O(5)	1.443(15)	O(4)–P(2)–O(5)	107.3(8)
P(2)–O(6)	1.523(14)	O(4)–P(2)–O(6)	107.1(7)
P(2)–O(7)	1.544(14)	O(4)–P(2)–O(7)	104.4(7)
		O(5)–P(2)–O(6)	113.6(9)
P(3)–O(8)	1.531(14)	O(5)–P(2)–O(7)	111.7(8)
P(3)–O(9)	1.493(13)	O(6)–P(2)–O(7)	112.0(7)
P(3)–O(10)	1.522(13)	O(8)–P(3)–O(9)	111.1(7)
P(3)–O(11)	1.603(14)	O(8)–P(3)–O(10)	110.0(7)
		O(8)–P(3)–O(11)	106.8(8)
P(4)–O(11)	1.625(13)	O(9)–P(3)–O(10)	114.8(8)
P(4)–O(12)	1.510(15)	O(9)–P(3)–O(11)	107.8(7)
P(4)–O(13)	1.531(14)	O(10)–P(3)–O(11)	105.7(7)
P(4)–O(14)	1.503(14)	O(11)–P(4)–O(12)	107.9(8)
		O(11)–P(4)–O(13)	106.6(7)
P(1)–O(4) –P(2)	130.0(9)	O(11)–P(4)–O(14)	103.8(7)
P(3)–O(11)–P(4)	132.1(8)	O(12)–P(4)–O(13)	113.0(8)
		O(12)–P(4)–O(14)	113.5(9)
		O(13)–P(4)–O(14)	111.3(8)

TABLE IV

DIHEDRAL ANGLES (°) FOR LEAD PYROPHOSPHATE

O(1) –P(1)–O(4) –P(2)	172.5(17)
O(2) –P(1)–O(4) –P(2)	55.4(20)
O(3) –P(1)–O(4) –P(2)	–66.0(20)
O(5) –P(2)–O(4) –P(1)	174.2(17)
O(6) –P(2)–O(4) –P(1)	51.8(21)
O(7) –P(2)–O(4) –P(1)	–67.1(20)
O(8) –P(3)–O(11)–P(4)	–59.9(22)
O(9) –P(3)–O(11)–P(4)	–179.4(14)
O(10)–P(3)–O(11)–P(4)	57.3(23)
O(12)–P(4)–O(11)–P(3)	49.9(23)
O(13)–P(4)–O(11)–P(3)	–71.7(22)
O(14)–P(4)–O(11)–P(3)	170.6(19)

squares refinement minimizing $\Sigma w(|F_0| - |F_c|)^2$, where the weighting factor (w) is $w = \sigma^{-2}(F_0)$, was employed. Final R factors are $R = 0.069$ and $R_w = 0.067$, where $R = \Sigma||F_0| - |F_c||/\Sigma|F_0|$ and $R_w = (\Sigma w||F_0| - |F_c||^2/\Sigma w|F_0|^2)^{1/2}$. Scattering factors and anomalous dispersion terms were obtained from the usual source (*17*). Experimental and statistical data are summarized in Table I. Atomic coordinates and bond distances and angles are given in Tables II and III. Dihedral angles for the P_2O_7 group are given in Table IV.

Discussion

Assignment of coordination numbers for the large divalent cations, Pb^{2+}, was made by geometric and distance considerations and through the application of the bond valence model (*18*). Table V shows the bond strengths calculated for $Pb_2P_2O_7$ from the bond strength curves of Brown and Wu (*19*). All distances less than 3.60 Å were considered in the calculations and the largest terms whose sums satisfied the valence requirements were kept. The summations of the bond valence values, the bond strength (BS), about each of the lead atoms are all within 4% of the ideal sum (valence equal 2). Pb(1) is perfectly satisfied and the bond strength sums related to the phosphorus and oxygen atoms are also reasonable (ideal sums are 5 and 2, respectively). The coordination numbers are 8 for Pb(1) and Pb(4) and 9 for Pb(2) and Pb(3). Pb(1) is coordinated to eight oxygen atoms arranged as a hybrid of D_{2d} and D_{4d} symmetries approximating a biaugmented trigonal prism. Pb(2) and Pb(3) are both nine-coordinated and have the geometric configuration of a distorted monocapped square antiprism. Pb(4) is bonded to eight oxygen atoms, best described as a severely distorted square antiprism. The experimental Pb–O interatomic distances for the eight- and nine-coordinated lead atoms ranged from 2.435 to 3.299 Å (mean distance 2.695 Å) and from 2.432 to 3.345 Å (mean distance 2.767 Å), respectively. Summing the lead and oxygen ionic radii obtained from the work of Shannon (*20*) yields the following calculated bond distances (observed values in parentheses) for Pb(1), Pb(2), Pb(3), and Pb(4), respectively: 2.665 (2.702), 2.721 (2.763), 2.721 (2.770), and 2.663 (2.688) Å. All of the lead atoms are linked together by μ-oxo bridges. Pb(1) and Pb(2) have four lead atom neighbors and Pb(3) and Pb(4) have five lead atom neighbors at distances ranging from 3.96 to 4.53 Å. This could be

TABLE V

BOND STRENGTHS (BS) FOR $Pb_2P_2O_7$ ($\times 10^3$)

	Pb(1)	Pb(2)	Pb(3)	Pb(4)	P(1)	P(2)	P(3)	P(4)	BS
O(1)	298	161	83		1363				1905
O(2)	305	155		204	1448				2112
O(3)	366			334	1176				1876
O(4)	122				936	1024			2082
O(5)			156	309		1651			2116
O(6)	349		130	140		1310			1929
O(7)	193			248		1235			2058
				382					
O(8)		249	314				1281		2014
			170						
O(9)	72	66	383				1427		1948
O(10)	295	264	143				1314		2016
O(11)		112					1052	992	2156
O(12)		342	217	102				1359	2020
O(13)		384	327					1281	1992
O(14)		258		230				1387	1875
BS	2000	1991	1923	1949	4923	5220	5074	5019	

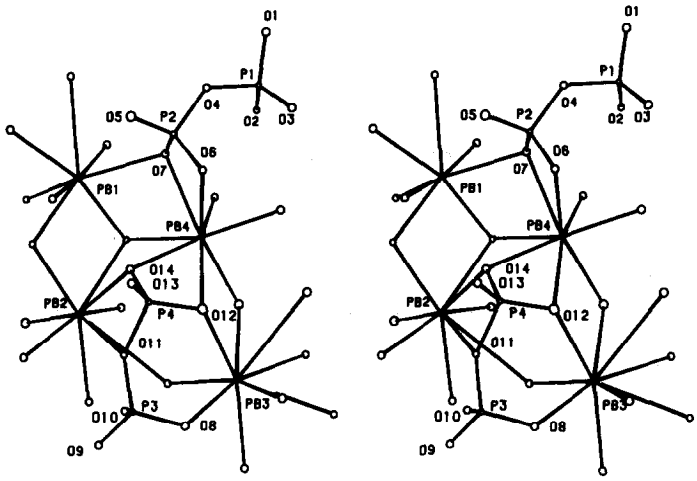

FIG. 1. Stereo view of the asymmetric unit of $Pb_2P_2O_7$. The lead atoms are shown fully coordinated.

an important element of lead coordination in lead phosphate glasses. A stereoview of the asymmetric unit with all the lead atoms fully coordinated is presented in Fig. 1.

The four unique phosphorus atoms are tetrahedrally coordinated (mean O–P–O angle 109.3°), and adjacent tetrahedra share one vertex to form distinct diphosphate groups. The P_2O_7 groups are repeated through lattice translations to form sheets which are shown in Fig. 2. The P_2O_7 group is eclipsed along the P–P axis. This eclipsing of the *Y–Y* axis is a distinction of the dichromate-type structure. The eclipsing dihedral angle of P_1–P_2 is 13.5(13)° and that of P_3–P_4 is 9.4(13)°. $Pb_2V_2O_7$ also has eight- and nine-coordinated Pb^{2+} ions and a divanadate group, V_2O_7, that is eclipsed to within 11° (*21*). The P–O bridging distances between P–O–P are longer than the P–O terminal distances as in the general case. The average of all P–O terminal distances is 1.513(30) Å, while the average P–O bridge distance is 1.622(19) Å. The numbers are reasonable when compared to the sum of radii given by Shannon, 1.55 Å (21). Brown and Calvo (*1*) have described the *Y*–O–*Y* angle of this dichromate-type compound as being 130°. The angles observed in our structural analysis of $Pb_2P_2O_7$ are P_1–O_4–P_2, 130.0(9)°, and P_3–O_{11}–P_4, 132.1(8)°. Other examples in the literature are 131 and 138° for β-$Ca_2P_2O_7$ (*22*) and 132° for $Cd_2P_2O_7$ (*8*).

Small-angle X-ray investigations of lead–iron phosphate and pure lead phosphate glasses are currently in progress and small-angle neutron scattering studies of these materials are planned. Additionally, Raman

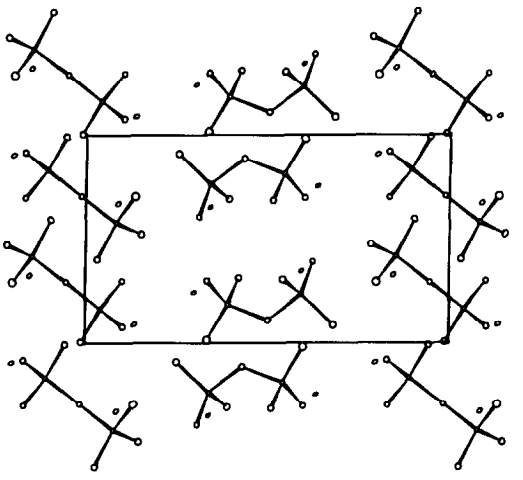

FIG. 2. An *ac* projection of the structure of $Pb_2P_2O_7$ is shown with the diphosphate groups drawn in. The typical dichromate-type sheets are present.

scattering and Mössbauer spectroscopy are being employed to gain additional insight into the structural properties of amorphous lead–iron phosphate. Hopefully, by combining these forthcoming results with those of the present structural study, some understanding of the nature of the structural relationships and transitions between amorphous and crystalline lead phosphates can be obtained.

Acknowledgments

This work was supported by The Robert A. Welch Foundation (Grant AA-668) and Baylor University.

References

1. I. D. Brown and C. Calvo, *J. Solid State Chem.* **1,** 173 (1970).
2. C. Calvo and K. Neelakantan, *Canad. J. Chem.* **48,** 890 (1970).
3. P. K. L. Au and C. Calvo, *Canad. J. Chem.* **45,** 2297 (1967).
4. Yu. I. Smolin and Yu. F. Shepelev, *Acta Crystallogr. Sect. B* **26,** 484 (1970).
5. J. K. Brandon and I. D. Brown, *Canad. J. Chem.* **46,** 933 (1968).
6. J. A. Baglio and J. N. Dann, *J. Solid State Chem.* **4,** 87 (1972).
7. R. D. Shannon and C. Calvo, *Canad. J. Chem.* **51,** 70 (1973).
8. C. Calvo and P. K. L. Au, *Canad. J. Chem.* **47,** 3409 (1969).
9. C. Calvo, *Inorg. Chem.* **7,** 1345 (1968).
10. Lars-Ove Hagman, I. Jansson, and C. Magneli, *Acta Chim. Scand.* **22,** 1419 (1968).
11. L. H. Brixner, P. E. Bierstedt, and C. M. Foris, *J. Solid State Chem.* **6,** 430 (1973).
12. B. C. Sales, M. M. Abraham, J. B. Bates, and L. A. Boatner, *J. Non-Cryst. Solids,* in press.
13. B. C. Sales and L. A. Boatner, *Science* **226,** 45 (1984).
14. B. C. Sales and L. A. Boatner, *Mater. Lett.* **2,** 301 (1984).
15. B. C. Sales and L. A. Boatner, *J. Non-Cryst. Solids,* in press.
16. P. Main, MULTAN 11/82, "A System of Computer Programs for the Automatic Solution of Crystal Structures from X-Ray Diffraction Data," University of York (1982).
17. "International Tables for X-Ray Crystallography," Vol. IV, Kynoch Press, Birmingham (1974).
18. I. D. Brown, *Acta Crystallogr. Sect. B* **33,** 1305 (1977).
19. I. D. Brown and K. K. Wu, *Acta Crystallogr. Sect. B* **32,** 1957 (1976).
20. R. D. Shannon, *Acta Crystallogr. Sect. A* **32,** 751 (1976).
21. R. D. Shannon and C. Calvo, *Canad. J. Chem.* **51,** 70 (1973).
22. N. C. Webb, *Acta Crystallogr.* **21,** 942 (1966).